An excellent crystal selected for measurement showed the following forms: c $\{0001\}$, m $\{10\bar{1}0\}$, a $\{11\bar{2}0\}$, q $\{30\bar{3}1\}$, and e $\{22\bar{4}1\}$.

The masses of arsenides in which the algodonite occurs are rich in copper near the matrix, and the arsenic content appears to increase in the centers of the masses. The good crystals line pockets in the arsenides; algodonite is interstitial to quartz and calcite and so does not form well-developed crystals in the matrix.

References

BUERGER, M. J. (1937) A common orientation and a classification for crystals based upon a marcasite-like packing. *Am. Mineral.* **22**, 48.

MOORE, P. B. (1962) Copper arsenides at Mohawk, Michigan. *Rocks and Minerals.* **37**, 24.

ON THE MICROSCOPIC DETERMINATION OF THE AMPHIBOLES IN GRAINS

PAOLO GAZZI, *Institute of Mineralogy and Petrography, Bologna University, Bologna, Italy.*

The optical identification of minerals in grains, as for instance is the case in the study of sands, is made easier in many cases by the use of cleavage plates which represent, in fact, sections having a definite crystallographic orientation. This method has been widely used for feldspars, but not for either monoclinic amphiboles or pyroxenes.

Experience shows that if either small amphiboles or pyroxenes crystals are crushed very carefully, in addition to the most commonly found plates parallel to the prism faces $\{110\}$, plates parallel to (100) are obtained in good number as well, whereas only in exceptional cases are plates parallel to (010) encountered, on which main extinction angle can be determined. In any event the cleavage plates have an elongated shape with two rectilinear sides parallel to the c crystallographic axis.

In order to ascertain with absolute certainty the fact that a plate lies perfectly parallel to a cleavage plane, it will be necessary to check whether it has flat faces and constant thickness values (better if thin), *i.e.* if it presents a uniform interference color (better when such color is rather low). Diminution of interference colors very close to the edges of the plate introduces no doubt.

After such control has been made, the distinction among the three types of cleavage is always possible through observation in convergent light:

(1) Plates parallel to (010) may be recognized by the centered emergence of a main axis of the indicatrix and by inclined extinction; such plates are absent however, as a rule.

(2) Plates parallel to (100) may readily be recognized by their parallel extinction and, through observation in convergent light, by the position normal to the plane of the plate and parallel to its elongation of a main section of the indicatrix (the optic plane in most cases); these plates permit determination of which axis of the indicatrix coincides with the b crystallographic axis, its refractive index and the birefringence sign.

(3) Cleavage plates parallel to (110), having inclined extinction, are oblique to all three main sections of the indicatrix. In amphiboles a main section of the indicatrix (the optic plane in most cases) is inclined 28° to the normal to the (110) plate, and this permits the control mentioned below through observation in convergent light. By rotating the crystal plate until the isogyres form the cross, the arm of the cross parallel to the c axis (elongation of the plate) will result in marked displacement as regards the center of the field. Such displacement is equal to about 9/10 of the radius of the field when an objective having a 0.85 N.A. is employed; to be more exact, and provided Mallard's formula may be applicable to the objective employed, such value will be equal to 88/100 when $n = 1.6$, 94/100 when $n = 1.7$.

The $c \wedge Z'$ extinction angle on the plate parallel to (110) can be used to advantage for diagnostic purposes. As direct determinations of this angle are not to be found in the literature, it will be necessary for the time being to calculate it on the basis of four known features: the nature of the axis of indicatrix coinciding with the b axis, the main extinction angle, the optic axial angle; and the angle between the normal to (110) and the b axis.

From Fresnel's construction it follows that on a section, no matter how oriented, and containing a reference axis, the extinction angle is equal to the half-sum of angles x_1 and x_2 included between the reference axis and the orthogonal projections of the two optic axes on the section itself.

In the monoclinic system, of particular interest are those cases in which the reference axis, lying inside the section under consideration, lies within a main section of the optic indicatrix as well. Some very simple formulae allowing a very fast calculation of the extinction angles may be obtained in such cases by expressing separately the values for x_1 and x_2.

In order to arrive at the determination of such formulae the application of known trigonometric relations, the same ones employed by Michel Levy (1888, p. 9–23) to obtain formulae expressing directly the extinction angles, will be sufficient. The formulae here derived are especially suited to emphasize the shape of the curves representing the variations of the extinction angle when the section is rotated around the reference axis; they are however exceedingly complicated for calculating the numerical values of the extinction angles.

In case 1) *i.e.* when the optic plane is parallel to (010), the formula coincides with the one obtained by Harker (1893), Daly (1899), and Tomita (*v.* Parker, 1961).

In cases 2) and 3) *i.e.* when the optic plane is normal to (010), the formula presented

here has never been used before and is far simpler and quicker than those previously employed.

$$c \wedge Z'_{(110)} = \tfrac{1}{2}(x_1 + x_2)$$

1) $Y\|b$ $\tan x_1 = \tan [(c \wedge Z) + V_z] \cos [b \wedge \perp (110)]$

       $\tan x_2 = \tan [(c \wedge Z) - V_z] \cos [b \wedge \perp (110)]$

2) $X\|b$ $\tan x_1 = \dfrac{\cos [b \wedge \perp (110)] \sin (c \wedge Z) + \sin [b \wedge \perp (110)] \tan V_z}{\cos (c \wedge Z)}$

       $\tan x_2 = \dfrac{\cos [b \wedge \perp (110)] \sin (c \wedge Z) - \sin [b \wedge \perp (110)] \tan V_z}{\cos (c \wedge Z)}$

3) $Z\|b$ by substituting X for Z the preceding formula yields the angle $c \wedge X'_{(110)}$.

In the case, by far the most common, in which the Y axis of the optic indicatrix coincides with the *b* crystallographic axis, the diagrams shown on Figs. 1 and 2 indicate the variations of the $c \wedge Z'$ extinction angle on (110) against the $c \wedge Z$ and 2V angles. The curves have been calculated for values of $c \wedge Z$ at 2° intervals.
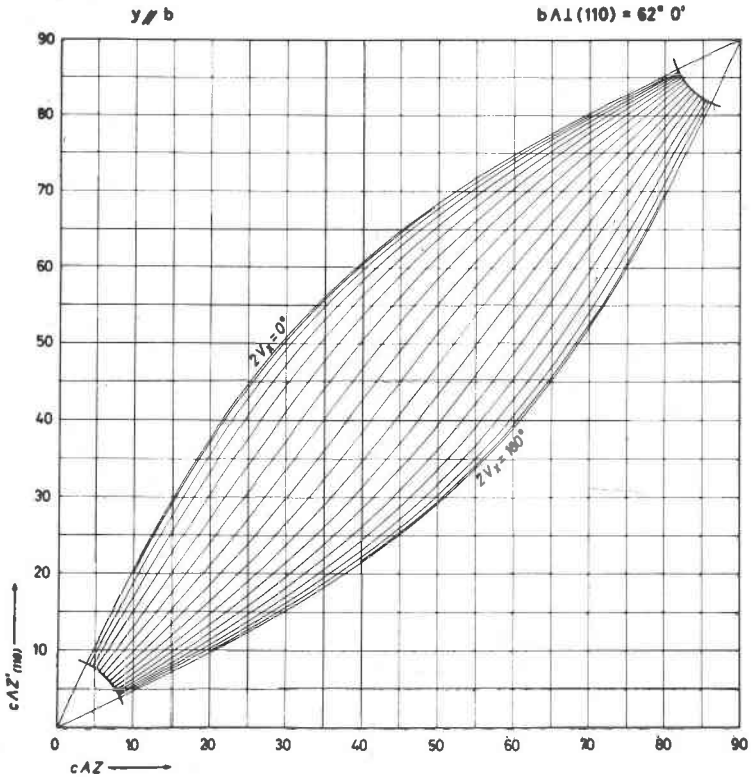

FIG. 1. Variations of $c \wedge Z'_{(110)}$ against $c \wedge Z$ and 2V angles on amphiboles. Curves for 2V are at 10° intervals ($2V_x = 0°, 10°, 20°, \ldots$ etc.).
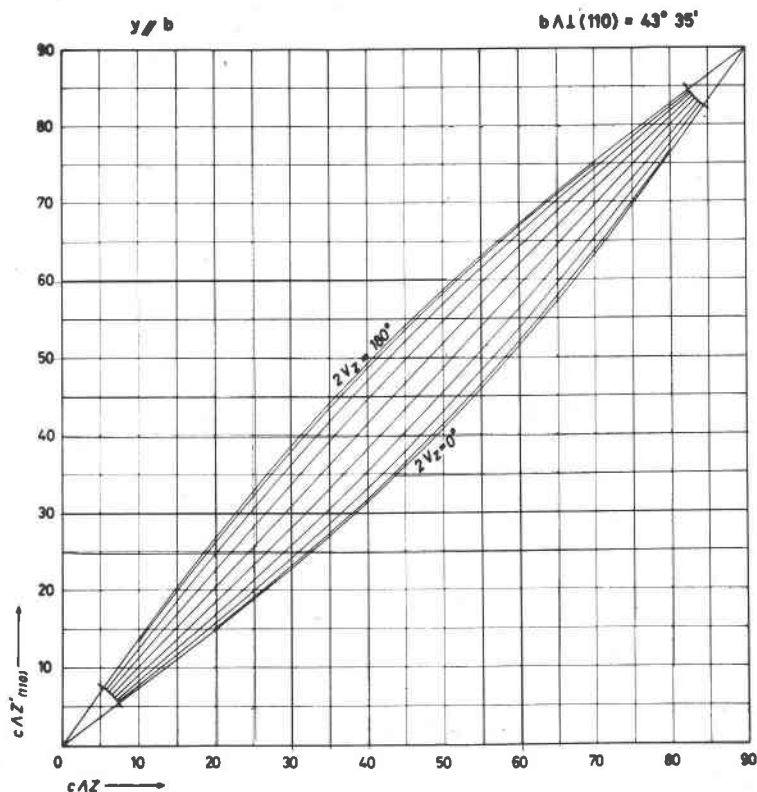
FIG. 2. Variations of $c \wedge Z'_{(110)}$ against $c \wedge Z$ and 2V angles on pyroxenes. Curves for 2V are at 20° intervals ($2V_z = 0°$, 20°, 40°, . . . etc.).

Angle $b \wedge \perp(110)$ varies but slightly in the different amphiboles, as well as in the different pyroxenes; such variations influence the values calculated for the $c \wedge Z'_{(110)}$ extinction angle only in a negligible way.

For amphiboles (Fig. 1) we have used $b \wedge \perp(110) = 62°0'$; for $b \wedge \perp(110) = 62°30'$ the greatest difference is for the values of $c \wedge Z = 56°$ and $2V_x = 180°$, $c \wedge Z'_{(110)}$ passing from 34°50' to 34°24'.

For pyroxenes (Fig. 2) we have used $b \wedge \perp(110) = 43°35'$; for $b \wedge \perp(110) = 44°30'$ the greatest difference is for the values of $c \wedge Z = 50°$ and $2V_z = 0°$, $c \wedge Z'_{(110)}$ passing from 40°48' to 40°22'.

Such differences, which are really much smaller in actual instances, do not exceed those due to experimental error incurred in determining an extinction angle, and therefore the curves may, in practice, be applied to all the members having Y‖b.

It may be observed that in amphiboles having the same $c \wedge Z$, the $c \wedge Z'_{(110)}$ angle varies greatly when 2V varies. In pyroxenes such varia-
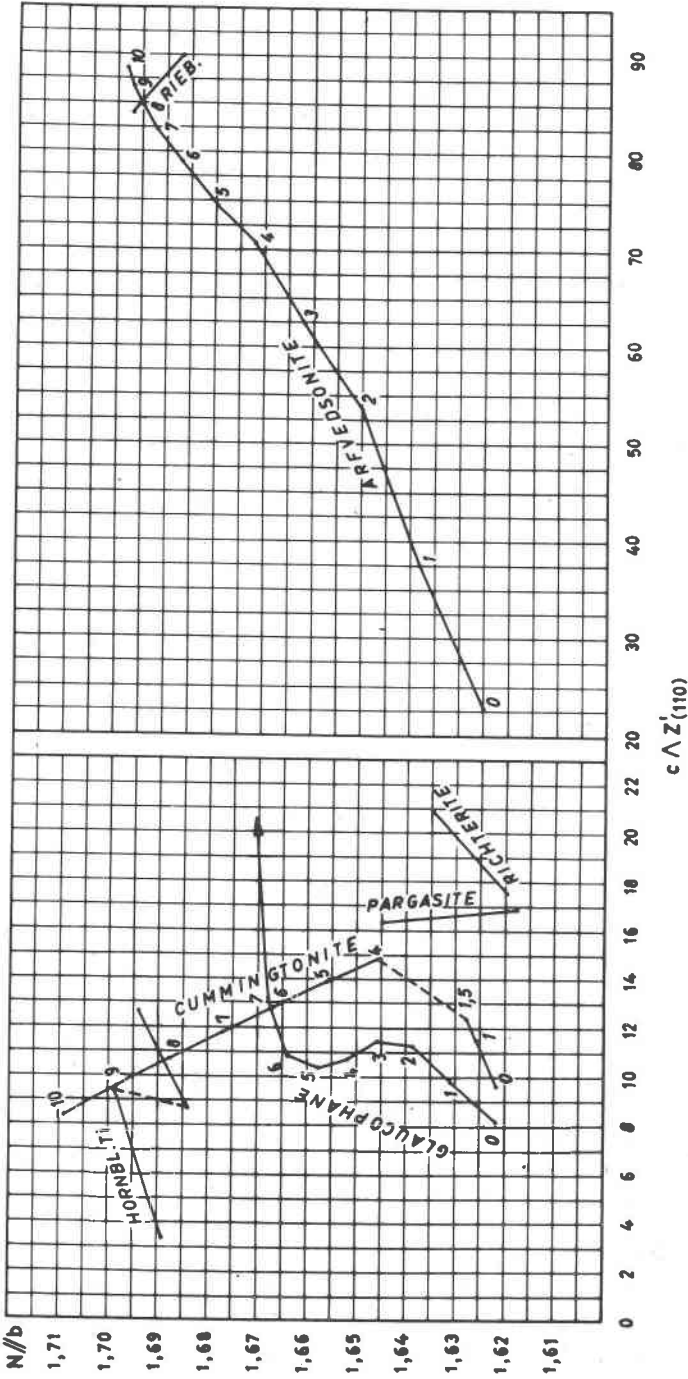
Fig. 3. Extinction angles $c \wedge Z'_{(110)}$ on titaniferous hornblendes, cummingtonites, glaucophanes, pargasites, richterites, arfvedsonites and riebeckites in terms of $N\|b$.

tion is considerably more limited, $c \wedge Z'_{(110)}$ is nearer $c \wedge Z$ and usually smaller, being $2V_z \leq 70°$, aegirine and aegirineaugite excepted.

It follows that it may prove more interesting to consider the values of $c \wedge Z'_{(110)}$ for the members of the different series of the amphiboles group than for pyroxenes.

Figure 3 and 4, calculated on the basis of the data quoted by Tröger (1956), show the variation of the $c \wedge Z'_{(110)}$ angle and that of the refractive index in the direction of the *b* axis in the different series of amphiboles. In the most ferriferous members of the glaucophane series, the extinction angle (not given in Fig. 3) becomes rapidly larger and has scant meaning, because the optic axes approach closely the normals to the prism faces {110}.

The diagnostic usefulness of the $c \wedge Z'_{(110)}$ extinction angle are equal, in general, to that of the $c \wedge Z$ angle and, in some particular cases, definitely greater.

Figure 4 and 5 show how the $c \wedge Z'_{(110)}$ angle allows a definite distinction among the actinolite, hornblende and hastingsite series, with an obvious diagnostic advantage, as no superimpositions occur for this angle, as happens for $c \wedge Z$.

The distinction is far less clear among the different members of the actinolite series.

A constant advantage of the use of the $c \wedge Z'_{(110)}$ angle as against $c \wedge Z$ lies in the following considerations:
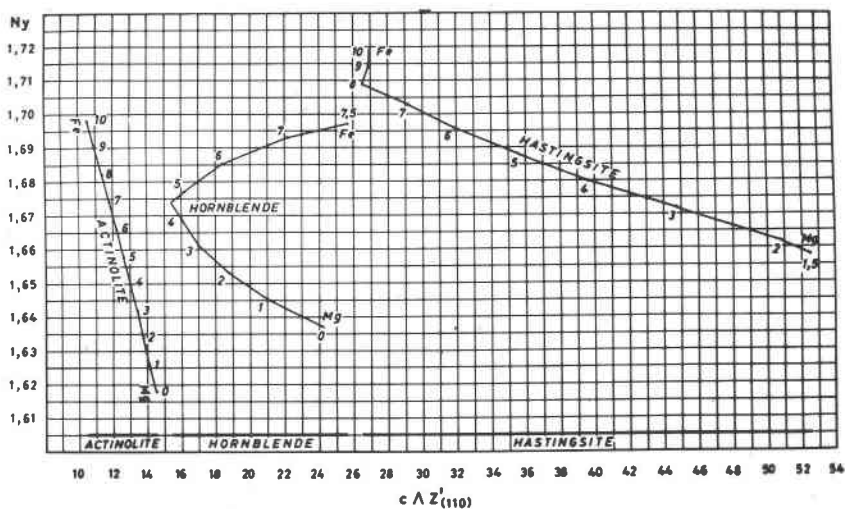

FIG. 4. Extinction angles $c \wedge Z'_{(110)}$ on actinolites, hornblendes and hastingsites in terms of N‖b (N_y).
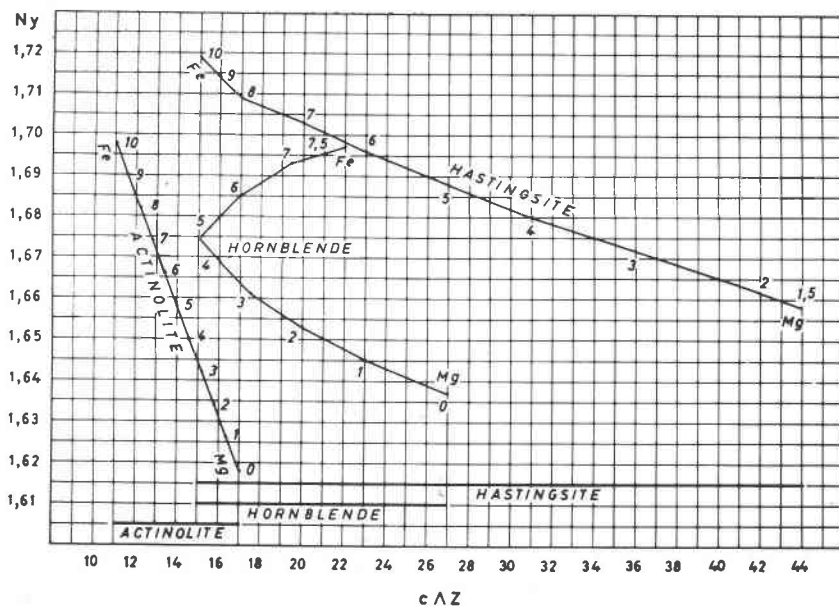
Fɪɢ. 5. Extinction angles $c \wedge Z$ on actinolites, hornblendes
and hastingsites in terms of N_y.

1) The angle $c \wedge Z$ may be determined, as a rule, only by means of the universal stage, and such a determination is liable to an error of about $3°–4°$, whereas on cleavage plates the extinction angle can be determined with an error of only about $1°$. 2) If one grain measuring 0.2 mm is crushed, many cleavage plates are obtained, and a large number of measurements may be taken in a far shorter time than that required for only one measurement with the universal stage.

Some disadvantage derives from the fact that the data determined directly on the amphiboles thus analyzed are not available, and that data calculated on the known values of $c \wedge Z$ and 2V can be influenced greatly by the sum of the errors affecting the primary data. We would suggest therefore that the complete study of each amphibole and pyroxene be accompanied by the determination of the extinction angle on the cleavage plates as well.

In practice, a satisfactory accord between the $c \wedge Z'_{(110)}$ values calculated and those determined directly on many members of the actinolite and hornblende series, as well as on some members of the hastingsite, cummingtonite and titaniferous hornblende series, has been obtained. The comparison has yielded less satisfactory results for different members of the glaucophane series, on which extinction angles smaller than the calculated ones have been determined; but in the cases taken into consideration the optic properties differ somewhat from those usually re-

ported, in particular lower values for $c \wedge Z$ and higher ones for $2V_x$ have been observed.

In a very recent paper, Parker (1961) presents, in separate diagrams, the curves relative to the extinction angle and refractive indexes on (110) for a number of different amphibole and pyroxene series, without pointing out however the advantages of this method. Some obvious inconsistencies result when Parker's data are compared with those that can be calculated from his primary data. This is especially true for the extinction angles of hornblendes having compositions near those of the endmembers, and of hastingsites having a prevalence of Fe^{2+} over Mg^{2+}; but also, for the whole glaucophane series for the greatest refractive index on (110), n_2, which results in smaller values than the index $\beta(N_y)$.

This study was carried out with the financial assistance of the Research Group, "Mineralogy of sediments," of the Italian Research Council (C.N.R.).

References

BURRI, C. (1950) *Das Polarisationsmikroskop*. Basel, 286–291.

DALY, R. A. (1899) On the optical characters of the vertical zone of the amphiboles and pyroxenes; and on a new method of determining the extinction angles of these minerals by means of cleavage pieces. *Proc. Am. Ac. Arts Sci.* **34**, 311–323.

HARKER, A. (1893) Extinction-angles in cleavage-flakes. *Mineral. Mag.* **10**, 239–240.

MICHEL-LEVY, A. (1888) Les minéraux des roches. 1, 9–23, Paris.

PARKER, R. B. (1961) Rapid determination of the approximate composition of amphiboles and pyroxenes. *Am. Mineral.* **46**, 892–900.

TRÖGER, W. E. (1956) *Optische Bestimmung der gesteinsbildenden. Minerale.* **1.** 65–77, Stuttgart.

DIMORPHIC RELATION IN Ag$_3$SbS$_3$

LUKE LI-YU CHANG, *Department of Geophysical Sciences, University of Chicago*

The dimorphic relation in Ag_3SbS_3 has not been well understood. In nature monoclinic pyrostilpnite is very rare, whereas rhombohedral pyrargyrite is described as an important and abundant ore of silver and formed at low temperatures (Palache *et al.*, 1952). Miers (Palache *et al.*, 1952), who first studied these two minerals, concluded that pyrargyrite and pyrostilpnite were always contemporaneous. Jensen (1947), in his study on the system $Ag_2S-Sb_2S_3$, stated that "the compound $3Ag_2S \cdot Sb_2S_3$ showed no heat effects below the melting point. This was unexpected, because this compound is formed in nature as two distinct mineral species, pyrargyrite and pyrostilpnite."

Pyrargyrite has been prepared previously by several methods (van